Variational Approach for Many-Body Systems at Finite Temperature

Tao Shi,[1,2] Eugene Demler,[3] and J. Ignacio Cirac[4,5]
[1]Institute of Theoretical Physics, Chinese Academy of Sciences, P.O. Box 2735, Beijing 100190, China
[2]CAS Center for Excellence in Topological Quantum Computation, University of Chinese Academy of Sciences, Beijing 100049, China
[3]Department of Physics, Harvard University, 17 Oxford Street, Cambridge, Massachusetts 02138, USA
[4]Max-Planck-Institut für Quantenoptik, Hans-Kopfermann-Strasse. 1, 85748 Garching, Germany
[5]Munich Center for Quantum Science and Technology (MCQST), Schellingstr. 4, D-80799 München, Germany

(Received 27 January 2020; revised 2 July 2020; accepted 18 September 2020; published 28 October 2020)

We introduce an equation for density matrices that ensures a monotonic decrease of the free energy and reaches a fixed point at the Gibbs thermal. We build a variational approach for many-body systems that can be applied to a broad class of states, including all bosonic and fermionic Gaussian, as well as their generalizations obtained by unitary transformations, such as polaron transformations in electron-phonon systems. We apply it to the Holstein model on 20×20 and 50×50 square lattices, and predict phase separation between the superconducting and charge-density wave phases in the strong interaction regime.

DOI: 10.1103/PhysRevLett.125.180602

In thermal equilibrium, the Gibbs state [1] can be obtained by using a purification [2] Φ and evolving a maximally entangled state according to

$$d_\tau|\Phi\rangle = -[H - h(\tau)]|\Phi\rangle, \tag{1}$$

for a time $\tau_T = 1/2T$, where H is the system Hamiltonian, and $h(\tau) = \langle\Phi|H|\Phi\rangle$. For many-body systems, doing this exactly is not possible due to the exponential growth of the number of necessary parameters with the system size. One way to overcome that is to restrict oneself to a family of states $\Phi(\xi)$ that is easy to describe and mimics the Gibbs state. One can then use the imaginary-time variational method (ITVM) [3] to determine $\xi(\tau)$ by restricting Eq. (1) to that family. This is the method of choice in tensor networks [4,5], where it has provided a useful description of many-body problems at finite temperature in one dimension.

A key feature of Eq. (1) is that the mean energy $h(\tau)$ monotonically decreases with τ. In the ITVM, this is inherited by the equations obeyed by $\xi(\tau)$ if one uses differential geometry methods to deduce them from Eq. (1) [6]. This is particularly useful for zero temperature studies [7], where ITVM becomes a truly variational method. At finite temperature, however, the Gibbs free energy is the right quantity to characterize the system. Unfortunately, Eq. (1) does not ensure that it decreases, and thus ITVM is not a truly variational method.

In this Letter, we introduce an equation that extends Eq. (1) to finite temperatures, ensuring that the free energy decreases with τ: regardless of the initial density operator, the system ultimately flows to the Gibbs ensemble. We use a purification to express it as in Eq. (1) and show how to apply it to families of states, obtaining a truly variational method which we call the free energy flow based variational method (FEFVM). It provides us with the natural extension of the standard ITVM for finite temperatures. We first apply our method to a textbook example to illustrate how it circumvents the limitations of ITVM. This is the Hubbard Model in two dimensions with attractive interactions, where standard mean-field methods provide a good description of the presence of superconductivity below a certain temperature [8]. We use both ITVM and FEFVM with Gaussian states that are the basis of mean-field theory. We explain why ITVM fails, and how FEFVM arrives at the correct mean-field results. We then apply FEFVM to the 2D Holstein model describing electrons on a lattice interacting with optical phonons. Here, simple mean-field analysis is not sufficient since it can capture the charge density wave (CDW), but not the superconducting order parameters. Furthermore, for strong electron-phonon interaction the phase diagram is challenging even for advanced numerical methods, such as quantum Monte Carlo or the analytic Migdal-Eliashberg solution. We predict that for a wide range of filling factors, sufficiently low temperature, and strong interactions a phase separation occurs between superconducting (SC) and CDW phases. While this model has been studied previously [9–13], the strong coupling regime has not been analyzed and the possibility of phase separation has not been considered. We attribute this to the fact that earlier papers have been limited in system sizes that could be investigated, an impediment that is absent in FEFVM, since we can use it to study systems with up to 50×50 sites. A summary of our results is shown in Fig. 1 with the resulting phase diagram for phonon frequency $\omega_b/t = 10$ and filling factor $\nu = 0.6$, where T is the temperature, g the coupling constant, and t the hopping energy. As expected [9–13], we predict a superconducting phase at low g. For higher g, it predicts separation between

 © 2020 American Physical Society

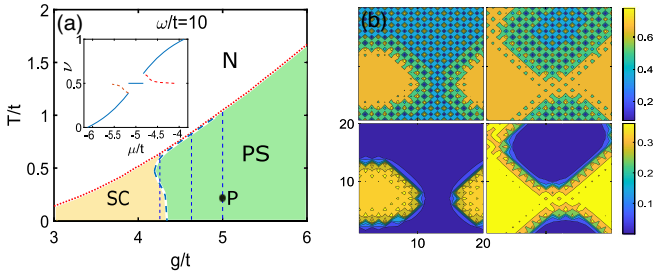

FIG. 1. (a) Phase diagrams for the Holstein model in a 50×50 lattice for $\omega_b/t = 10$ and $\nu = 0.6$. The inset displays the filling factor ν as a function of the chemical potential at the point P, where $g/t = 5$, $T/t = 0.2$. (b) Phase separations at P for $\nu = 0.56$ (left panel) and $\nu = 0.6$ (right panel) in a 20×20 lattice. The first and second rows display the electron density and the SC order parameter.

the SC and CDW phases. This is obtained by both a homogeneous and a general variational ansatz. This follows from the negative value of the compressibility [Fig. 1(a)], and the distribution of the electron density and the SC order parameter [Fig. 1(b)], respectively. The CDW transition temperature monotonically increases with increasing g. This should be understood as the pseudogap temperature of the onset of short-range correlations because we used a variational family that does not fully account for vortex excitations. We expect, however, that it accurately describes the increasing temperature of phase separation.

Flow equation: Given a Hamiltonian H and a temperature T we are interested in the Gibbs state

$$\rho_T = e^{-\beta H}/Z, \tag{2}$$

where $Z = \mathrm{tr}(e^{-\beta H})$, and $\beta = 1/T$. A unique feature is that it minimizes the free energy functional

$$f(\rho) = \mathrm{tr}(H\rho) - TS(\rho), \tag{3}$$

where $S(\rho) = -\mathrm{tr}[\rho \ln(\rho)]$. The minimum of f is reached for $\rho = \rho_T$, so that this provides us with the variational principle. This minimization can be done through a flow equation that extends Eq. (1),

$$d_\tau \rho = -\{F(\rho) - f(\rho), \rho\}, \tag{4}$$

where the free energy operator $F(\rho) = H + T \ln \rho$, so that $f(\rho) = \mathrm{tr}[\rho F(\rho)]$, and $\{,\}$ denotes the anticommutator.

We now prove that the free energy monotonically decreases with τ, i.e., $d_\tau f[\rho(\tau)] \leq 0$ with the equality only if $\rho = \rho_T$ and that any initial (normalized) state $\rho(0)$ flows to ρ_T in the limit $\tau \to \infty$. From the definition of $f(\rho)$, we have $d_\tau f(\rho) = \mathrm{tr}(F d_\tau \rho) + T\mathrm{tr}(\rho d_\tau \kappa)$, where $\kappa \equiv \ln \rho$. The last term vanishes, since

$$\begin{aligned}\mathrm{tr}(\rho d_\tau \kappa) &= \mathrm{tr}\left[\int_0^1 du e^{(1-u)\kappa}(d_\tau \kappa) e^{u\kappa}\right] \\ &= \mathrm{tr}(d_\tau e^\kappa) = \mathrm{tr}(d_\tau \rho) = 0,\end{aligned}$$

where we have utilized that Eq. (4) conserves the trace of ρ. Using Eq. (4)

$$d_\tau f(\rho) = -2\mathrm{tr}[\rho X(\rho)^2] \leq 0, \tag{5}$$

where $X(\rho) = [F(\rho) - f(\rho)]$. The derivative vanishes when $X(\rho) = 0$ which leads to Eq. (2) [14].

We now transform Eq. (4) into an equation analogous to Eq. (1). We employ a particular purification of ρ, Φ_p (thermal double [2]). This is done by adding for each (bosonic or fermionic) mode an auxiliary one so that

$$|\Phi_p\rangle = (\sqrt{\rho} \otimes \mathbb{1})|\Phi^+\rangle, \tag{6}$$

where Φ^+ is a maximally entangled state between each mode and the corresponding auxiliary one [15], so that we can recover $\rho = \mathrm{tr}_a(|\Phi_p\rangle\langle\Phi_p|)$. It follows Eq. (4) that

$$d_t|\Phi_p\rangle = -[F_p(\Phi_p) - f_p(\Phi_p)]|\Phi_p\rangle, \tag{7}$$

where $F_p(\Phi) = F(\rho) \otimes \mathbb{1}$ and $f_p(\Phi) = f(\rho)$, with $\rho = \mathrm{tr}_a(|\Phi\rangle\langle\Phi|)$. The similarity of Eqs. (7) and (1) is apparent, although F_p depends on Φ and only acts nontrivially on the system. Thus, the resulting equation is nonlinear.

Variational method.—The success of variational methods crucially depends on the choice of variational states: they have to faithfully represent the physical behavior of the system under study and be amenable to an efficient computation of the observables of interest. A sensible choice is the set of Gaussian states, corresponding to density operators that can be written as a Gaussian function of the creation and annihilation operators. They underlie mean-field theories and the expectation values of observables can be efficiently computed by means of Wick's theorem. However, they are not able to represent some important phenomena; in particular, they cannot account for correlations between bosonic and fermionic degrees of freedom. Analogously to the zero temperature case [6], in order to circumvent this deficit, we use an extended family of states of the form

$$\rho_v(\xi) = U(\xi_u)\rho_G(\xi_g)U(\xi_u)^\dagger. \tag{8}$$

Here, ρ_G is an arbitrary Gaussian mixed state parametrized by ξ_g with $\mathrm{tr}(\rho_G) = 1$. U is a unitary operator which entangles different degrees of freedom and allows us to describe states that do not obey Wick's theorem. We take the family of unitary operators $U \in \mathcal{U}$ defined in the zero temperature case in Ref. [6]. The number of variational parameters scales polynomially with the system size.

With the goal of describing states in Eq. (8) we consider a purification,

$$|\Psi_v(\xi)\rangle = [U(\xi_u) \otimes \mathbb{1}]|\Psi_G(\xi_g)\rangle, \tag{9}$$

with a normalized pure Gaussian state Ψ_G so that $\rho_v(\xi) = \mathrm{tr}_a(|\Psi_v(\xi)\rangle\langle\Psi_v(\xi)|)$, where the trace is taken with respect to the ancilliary degrees of freedom [16].

Starting from Eq. (7) we derive in Ref. [17] a set of differential equations for the variational parameters of the purification $\xi(\tau)$. As announced, those equations inherit the important feature of the original flow equation (4), namely, that the free energy of $\rho_v[\xi(\tau)]$ monotonically decreases with τ. The main idea consists of projecting Eq. (7) onto the tangent plane of the manifold (9). The set $\mathcal{U}$ should be chosen so that this can be done efficiently. A feature of the chosen family of variational states is that the free energy operator F can be efficiently computed, since $\ln \rho_v = U(\xi_u) \ln[\rho_G(\xi_g)] U(\xi_v)^\dagger$, and the logarithm of a Gaussian state can be readily calculated [17].

As for ξ_g, we use the covariant matrix formalism. We consider N_b (N_f) bosonic (fermionic) modes with annihilation operators b_n (c_m). For a Gaussian state we take, as usual [17,20,21], the covariance matrix $\Gamma_{b,m}$ for the bosons and fermions, respectively, and the displacement vector, Δ_R [17].

Negative-U Hubbard model.—Let us briefly illustrate how the variational method overcomes some of the problems encountered by ITVM with a simple model,

$$H_{\mathrm{BCS}} = -t \sum_{\langle nm\rangle,\sigma} c^\dagger_{n\sigma} c_{m\sigma} + U \sum_n c^\dagger_{n\uparrow} c^\dagger_{n\downarrow} c_{n\downarrow} c_{n\uparrow}, \tag{10}$$

on a square lattice, where $\langle nm\rangle$ denotes nearest neighbor sites. It is well known that mean field BCS theory correctly describes the appearance of a SC phase at sufficiently low temperatures [22].

We compare the results of our method with ITVM (see also Ref. [17]). In both, we use the simple Fermionic Gaussian family of translationally invariant states [i.e., $(\Gamma_m)_{n,n'} = (\Gamma_m)_{n-n'}$], which are also the ones that underlie mean-field descriptions of this model. In this way, we can check if the flow equations [Eq. (1) for ITVM and Eq. (4) for FEFVM] converge to the correct mean-field result. To account for the spontaneous symmetry breaking in the SC phase, in the ITVM we introduce a small symmetry breaking in the Hamiltonian $\epsilon \sum_n c^\dagger_{n,\uparrow} c^\dagger_{n,\downarrow}$ and take $\epsilon \ll 1$.

In Fig. 2 we draw the s-wave order parameter, $\Delta_s = U|\langle c_{n\downarrow} c_{n\uparrow}\rangle|$, as a function of the temperature at half filling. The inset of Fig. 2 clearly shows that ITVM gives rise to an ϵ-dependent order parameter and free energy, and an incorrect critical temperature. In contrast, FEFVM correctly converges to the mean-field result. The reason for the failure of ITVM can be summarized as follows: the error accumulates along the time evolution up to the time $\tau = \beta/2$. This can be explicitly shown for the BCS model

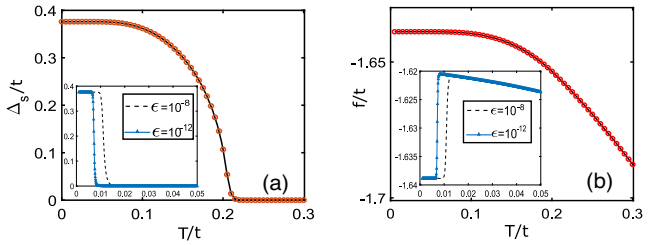

FIG. 2. Lattice BCS model: s-wave order parameter (a) and free energy density (b) as a function of the temperature T/t, for $U/t = -2$ and a 50×50 lattice at half filling. The red curve gives the result of the FEFVM, which is on top of the mean field result in the thermodynamic limit. The black dashed line and the green curve (see insert) correspond to the ITVM for a symmetry-breaking field with $\epsilon = 10^{-8}$, 10^{-12}, respectively.

[17]. However, for the FEFVM, ρ_T is a fixed point of Eq. (4) at $\tau \to \infty$, and does not depend on the path used to reach it. Furthermore, the ITVM does not perform well whenever there is symmetry breaking: Since the initial infinite-T thermal state maintains all symmetries during the flow, a small symmetry breaking has to be introduced. As the figure displays, the result provided by that method is very sensitive to the value of ϵ. This simple example illustrates that for finite temperature, a method that ensures the decrease of the free energy performs better than one based on imaginary time evolution, as it is used in the context of tensor networks [4].

Holstein model.—We now investigate the 2D Holstein model, which describes electrons on a lattice interacting with optical phonons. The Hamiltonian is $H = H_e + H_{\mathrm{ph}} + H_{\mathrm{int}}$, where

$$H_e = -t \sum_{\langle n,m\rangle,\sigma} c^\dagger_{n\sigma} c_{m\sigma},$$
$$H_{\mathrm{ph}} = \omega_b R^T R/4 - \omega_b/2,$$
$$H_{\mathrm{int}} = g \sum_{n\sigma} x_n c^\dagger_{n\sigma} c_{n\sigma},$$

with t, ω_b, and g, the electron hopping, phonon frequency, and coupling, respectively. For weak electron phonon-interaction, $g \ll \omega_b$, one can eliminate the bosons and obtain the negative-U Hubbard model. In that limit, at sufficient low temperatures the model displays a SC phase. For strong interactions and classical phonons, Esterlis *et al.* [9] have used a Monte Carlo analysis to predict a commensurate CDW behavior that can be understood as the localized phase of bipolarons. The CDW transition temperature has also been obtained via the determinantal quantum Monte Carlo method [10], which can be applied beyond the classical phonon limit but requires more computational resources. Most of the studies so far have worked at half filling, $\nu = 0.5$, where the total number of electrons coincides with the number of lattice sites.

We study the 2D Holstein model in both the weak- and strong-coupling regime using the variational ansatz (9). In order to describe the electron-phonon correlations, we include a unitary transformation $U = e^S$, where $S = i\sum_{ln,\sigma} \lambda_{ln} p_l c^\dagger_{n\sigma} c_{n\sigma}$ contains the variational parameters λ_{ln}, in addition to those of the Gaussian states Δ_R and $\Gamma_{b,m}$. It is inspired by the Lang-Firsov transformation [23], but possess a high degree of flexibility to account for different phenomena [6]. We use two different *Ansätze* for Δ_R, $\Gamma_{b,m}$, and λ_{ln}: (i) General, where all components of the vector Δ_R and matrices Γ_b, Γ_m, and λ can take arbitrary values; (ii) Homogeneous, where $\Delta_{R,l} = \Delta_{R,0} + (-1)^l \Delta_{R,\pi}$ and $\xi_{n,n'} = \xi_{0,n-n'} + (-1)^n \xi_{\pi,n-n'}$, with $\xi = \Gamma_b, \Gamma_m, \lambda$. We can describe not only states with translational symmetry, but also with CDW orders.

In Fig. 1(a), we show the phase diagram for $\nu = 0.6$ and $\omega_b/t = 10$. Even though ω_b is large compared to t, the coupling constant g/t ranges from 3 to 6, which allows us to explore some intriguing physics in both the weak and strong coupling regimes. The phase diagram for a smaller phonon frequency is shown in Ref. [17]. As expected, for relatively small g and low temperatures we find a SC phase. As g increases, the full variational *Ansatz* (i) predicts phase separation between SC and a CDW phase. While the naive *Ansatz* (ii) predicts a supersolid phase (with nonvanishing SC and CDW order parameters), where both the SC order parameters $\Delta_{k=0,\pi} = \sum_n e^{-ikn} V_{nn} \langle c_{n\downarrow} c_{n\uparrow} \rangle / N$ ($V_{nn} = 2(\omega_b \sum_l \lambda_{ln}^2 - 2g\lambda_{nn})$ is introduced in Ref. [17] with momenta 0 and π exist, as shown in the left column of Fig. 3. The general *Ansatz* (i) establishes the presence of phase separation, as it is shown by the snapshots of the density distribution and the SC order parameter in Fig. 1(b) for fill factors $\nu = 0.56$ and 0.6. One can recover this later behavior from (ii) as well by two equivalent manners. The first relies on the fact that a negative value of the compressibility $\kappa = \partial_\nu^2 f$ indicates the onset of phase separation. In Fig. 3(b), κ is shown for $g/t = 4.3$, 4.7, and 5 as a function of T, which agrees with the corresponding region of phase diagram of Fig. 1(a) (cf. the three vertical lines). Alternatively, one can compute the chemical potential μ as a function of ν. As shown in Fig. 3(d) for $g/t = 5$ and $T/t = 0.2$ in a 50×50 lattice [see also the inset of Fig. 1(a)], in the interval $\nu \sim [0.3, 0.7]$, the $\mu - \nu$ diagram displays the phase separation between a CDW at half filling, and a SC phase. The same result follows from the Maxwell construction [19]. To carry it out, one plots the free energy $f_s = f + 4g^2\nu/\omega_b$ (extracting the phonon energy) as a function of ν, as shown in Fig. 3(d), and draws straight lines that are tangent to the free energy f and go through the minimum of f (which occurs at half filling). The fractions of CDW and SC phases, e.g., about 70% CDW (30 percent SC) at $\nu = 0.56$ and 50% CDW (50% SC) at $\nu = 0.6$, can be predicted by MC, which is in a very good agreement with the result [Fig. 1(b)] of the full variational *Ansatz* (i).

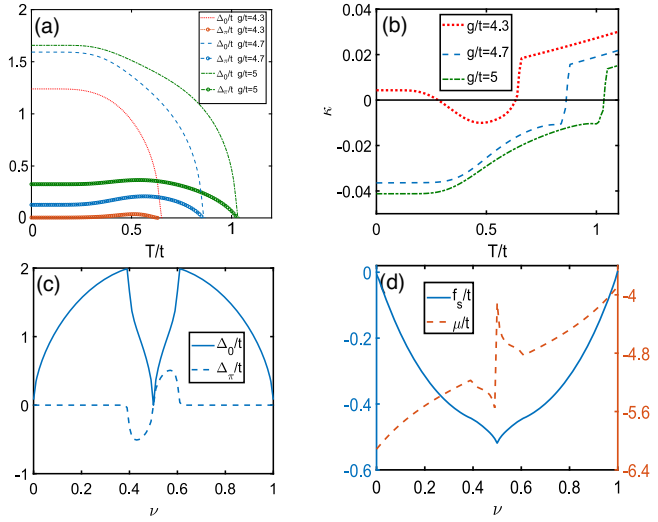

FIG. 3. (a)–(b) The SC order parameters and the compressibility along three vertical lines in Fig. 1 obtained using homogeneous *Ansätze*. Negative compressibility indicates thermodynamically unstable states and corresponds to phase separation. (c)–(d) The SC order parameters, the free energy, and the chemical potential versus the filling factor ν for $\omega_b/t = 10$, $g/t = 5$, $T/t = 0.2$. In (d) the free energy is plotted by subtracting a term proportional to the electron density, which does not affect the compressibility and the Maxwell construction. All plots have been obtained with the homogeneous *Ansatz*.

Conclusions.—We have introduced a flow equation that ensures that the free energy monotonically decreases and converges to the Gibbs state. This can be applied to the description of many-body systems within families of states, yielding an efficient method to find variational approximations to the Gibbs state. As compared to the methods based on an evolution in imaginary time, ours has the target state as a fixed point. We have applied it to Holstein models describing the interactions of electrons and phonons in a lattice. As compared to previous studies, we can deal with much larger system sizes, although the other methods can have other advantages when analyzing smaller systems. For strong coupling, we predict phase separation between a commensurate CDW at half filling and a SC phase with either lower or higher density, depending on whether the average density is below or above half filling. Otherwise, our findings are consistent with the results obtained by the Monte Carlo analysis in the model with classical phonons [9]. Our formalism can be extended to study broader classes of electron-phonon models, including the Migdal-Eliashberg regime with $\omega_b < t$, systems with both electron-electron and electron-phonon interactions, and systems with disorder. It can also be extended to compute spectral function [17] and to other families of variational states. In particular, it would be very interesting to adapt it for tensor networks to complement current methods in the study of finite temperatures.

We thank I. Esterlis, Y. Wang, and R. Scalettar for stimulating discussions. T. S. acknowledges the support from NSFC 11974363. J. I. C acknowledges the ERC Advanced Grant QENOCOBA under the EU Horizon2020 program (Grant Agreement No. 742102) and the German Research Foundation (DFG) under Germany's Excellence Strategy through Project No. EXC-2111-390814868 (MCQST) and within the D-A-CH Lead-Agency Agreement through Project No. 414325145 (BEYOND C). E. D. acknowledges support from Harvard-MIT CUA, ARO Grant No. W911NF-20-1-0163, the National Science Foundation through Grant No. OAC-1934714, AFOSR-MURI: Photonic Quantum Matter Award No. FA95501610323.

[1] K. Huang, *Statistical Mechanics*, 2nd ed. (John Wiley & Sons, New York, 1987).
[2] P. Martin and J. Schwinger, Phys. Rev. **115**, 1342 (1959); J. Schwinger, J. Math. Phys. (N.Y.) **2**, 407 (1961).
[3] P. A. M. Dirac, Proc. Cambridge Philos. Soc. **26**, 376 (1930); P. W. Langhoff, S. T. Epstein, and M. Karplus, Rev. Mod. Phys. **44**, 602 (1972).
[4] F. Verstraete, J. J. García-Ripoll, and J. I. Cirac, Phys. Rev. Lett. **93**, 207204 (2004); M. Zwolak and G. Vidal, Phys. Rev. Lett. **93**, 207205 (2004); S. R. White, Phys. Rev. Lett. **102**, 190601 (2009); E. M. Stoudenmire and S. R. White, New J. Phys. **12**, 055026 (2010); R. Orus, Nat. Rev. Phys. **1**, 538 (2019); P. Czarnik, J. Dziarmaga, and A. M. Oleś, Phys. Rev. B **93**, 184410 (2016); P. Czarnik, M. M. Rams, and J. Dziarmaga, Phys. Rev. B **94**, 235142 (2016); A. Kshetrimayum, M. Rizzi, J. Eisert, and R. Orus, Phys. Rev. Lett. **122**, 070502 (2019); S. S. Jahromi and R. Orus, arXiv:2005.00314.
[5] U. Schollwoeck, Ann. Phys. (Amsterdam) **326**, 96 (2011).
[6] T. Shi, E. Demler, and J. I. Cirac, Ann. Phys. (Amsterdam) **390**, 245 (2018); L. Hackl, T. Guaita, T. Shi, J. Haegeman, E. Demler, and J. I. Cirac, arXiv:2004.01015.
[7] Y. Ashida, T. Shi, M. C. Bañuls, J. I. Cirac, and E. Demler, Phys. Rev. Lett. **121**, 026805 (2018); P. Sala, T. Shi, S. Kühn, M. C. Bañuls, E. Demler, and J. I. Cirac, Phys. Rev. D **98**, 034505 (2018).
[8] R. T. Scalettar, E. Y. Loh, J. E. Gubernatis, A. Moreo, S. R. White, D. J. Scalapino, R. L. Sugar, and E. Dagotto, Phys. Rev. Lett. **62**, 1407 (1989); R. R. dos Santos, Phys. Rev. B **46**, 5496 (1992); R. R. dos Santos, Phys. Rev. B **48**, 3976 (1993); T. Paiva, R. R. dos Santos, R. T. Scalettar, and P. J. H. Denteneer, Phys. Rev. B **69**, 184501 (2004).
[9] I. Esterlis, S. A. Kivelson, and D. J. Scalapino, Phys. Rev. B **99**, 174516 (2019).
[10] M. Weber and M. Hohenadler, Phys. Rev. B **98**, 085405 (2018).
[11] F. Marsiglio, Phys. Rev. B **42**, 2416 (1990).
[12] R. M. Noack, D. J. Scalapino, and R. T. Scalettar, Phys. Rev. Lett. **66**, 778 (1991).
[13] M. Vekić, R. M. Noack, and S. R. White, Phys. Rev. B **46**, 271 (1992).
[14] Strictly speaking, this is the only solution as long as we impose that ρ has full rank. While we refer to Eq. (4) as imaginary time flow, it does not correspond to the analytic continuation of the real-time evolution.
[15] For the bosonic case, the state Φ^+ is not normalizable. However, since we use the covariant matrix formalism, this problem can be easily circumvented.
[16] One could also add another $U \in \mathcal{U}$ acting on the ancilla and depending on other variational parameters, as well as use a more symmetrized version of Eq. (7); see Ref. [17].
[17] See Supplemental Material at http://link.aps.org/supplemental/10.1103/PhysRevLett.125.180602 for the monotonicity of free energy, Gaussian thermal states, conservation law in EOM, imaginary and real-time EOM through purification, and the derivation of EOM for the Holstein model, which includes Refs. [6,18,19].
[18] T. Shi, J. I. Cirac, and E. Demler, Phys. Rev. Research **2**, 033379 (2020).
[19] L. E. Reichl, *A Modern Course in Statistical Physics*, 4th ed. (Wiley-VCH, New York, NY, 2016).
[20] D. Walls and G. Milburn, *Quantum Optics* (Springer, Berlin, 1994).
[21] K. E. Cahill and R. J. Glauber, Phys. Rev. A **59**, 1538 (1999).
[22] The mean-field approach is known to be quantitatively correct in the thermodynamic limit, although in one- and two-dimensional systems the transition temperature should be understood as that of opening of the quasiparticle gap, rather than the onset of the true long-range order.
[23] I. G. Lang and Y. A. Firsov, Zh. Eksp. Teor. Fiz. **43**, 1843 (1962).